

# CHEMBIOCHEM

## Supporting Information

© Copyright Wiley-VCH Verlag GmbH & Co. KGaA, 69451 Weinheim, 2010

### Targeted Photoswitchable Probe for Nanoscopy of Biological Structures

Claudio Dellagiacoma,<sup>[a]</sup> Gražvydas Lukinavičius,<sup>[b]</sup> Noelia Bocchio,<sup>[a]</sup> Sambashiva Banala,<sup>[b]</sup> Stefan Geissbühler,<sup>[a]</sup>  
Iwan Märki,<sup>[a]</sup> Kai Johnsson,<sup>\*[b]</sup> and Theo Lasser<sup>\*[a]</sup>

cbic\_201000189\_sm\_miscellaneous\_information.pdf

## 1. Chemical synthesis

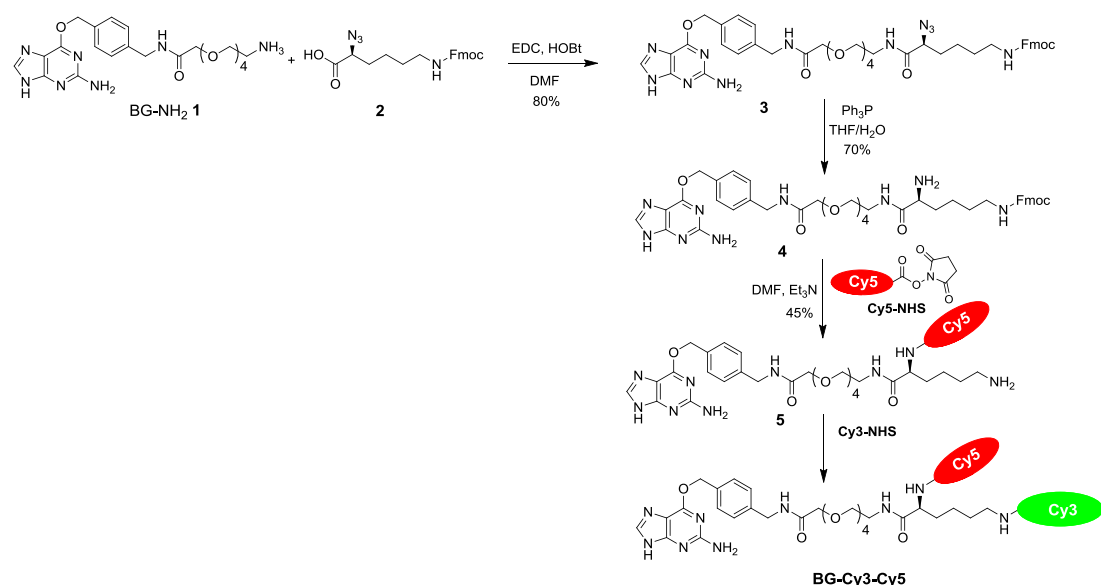


**Figure S1. Synthesis of BG-Cy3-Cy5**

Compounds **1**<sup>[1]</sup> and **2**<sup>[2]</sup> in Figure S1 were synthesized as previously described in the corresponding references.

**Synthesis of compound 3.** To a mixture of BG-NH<sub>2</sub> **1** (100 mg, 0.2 mmol) and lysine derivative **2** (78 mg, 0.2 mmol) in dry DMF (2 mL) were added N-(3-dimethylaminopropyl)-N'-ethylcarbodiimide hydrochloride (EDC, 96 mg, 0.5 mmol) and 1-hydroxybenzotriazole (HOBT, 67 mg, 0.5 mmol), and the resulting mixture was stirred for 1 h at room temperature. Water (30 mL) was added to the reaction mixture and extracted with AcOEt (2 x 30 mL). The organic phase was dried over Na<sub>2</sub>SO<sub>4</sub> and the solvent was removed *in vacuo*. The product was purified by flash column chromatography (4-10% MeOH in CH<sub>2</sub>Cl<sub>2</sub>). Yield: 140 mg (0.16 mmol, 80 %). MS(ESI) (m/z):[M+H]<sup>+</sup> calc for C<sub>44</sub>H<sub>54</sub>N<sub>11</sub>O<sub>9</sub>880.41; found 880.34.

**Synthesis of compound 4.** To a solution of compound **3** (25 mg, 28.4 μmol) in a solvent mixture of THF (1 mL) and water (50 μL) was added Ph<sub>3</sub>P (22 mg, 85.2 μmol) and the mixture was stirred overnight at room temperature. Solvents were removed *in vacuo* and the residue was redissolved in DMF. The product was purified by HPLC. Yield: 17 mg (17.9 μmol, 70%). <sup>1</sup>H NMR (400 MHz, DMSO-d<sub>6</sub>): 8.30 (q, *J* = 6.4 Hz, 1H), 7.92-7.81 (m, 4H), 7.73-7.55 (m, 4H), 7.46-7.39 (m, 4H), 7.34-7.27 (m, 4H), 6.28 (s, 1H), 6.25 (brs, 2H), 5.45 (s, 2H), 4.32 (d, *J* = 5.7 Hz, 2H), 4.28 (d, *J* = 6.4 Hz, 2H), 4.20 (t, *J* = 6.4 Hz, 1H), 3.94 (brs, 3H), 3.60-3.53 (m, 14H), 3.09 (t, *J* = 6.6 Hz, 2H), 2.95 (q, *J* = 5.8 Hz, 2H), 1.57-1.48 (m, 1H), 1.40-1.20 (m, 6H). HRMS-ESI (m/z):[M+2H]<sup>2+</sup> calc for C<sub>44</sub>H<sub>57</sub>N<sub>9</sub>O<sub>9</sub> 427.7134; found : 427.7152.

**Synthesis of compound 5.** To a solution of compound **4** (3 mg, 3.52  $\mu\text{mol}$ ) in dry DMF (0.5 mL) were added Cy5-NHS ester (1 mg, 1.26  $\mu\text{mol}$ ) and  $\text{Et}_3\text{N}$  (1  $\mu\text{L}$ ) and the reaction was continued overnight. The reaction was stopped by addition of few drops of water. (Note: As the amine **4** is present in excess, deprotection of Fmoc group occurred during the reaction). The product was purified by HPLC. Yield: 0.7 mg (45%) (determined by the extinction coefficient of Cy5,  $\epsilon_{647} = 250,000 \text{ M}^{-1} \text{ cm}^{-1}$  in pH 7.4 buffer). HRMS-ESI ( $m/z$ ):  $[\text{M}+\text{H}]^{2+}$  calc for  $\text{C}_{62}\text{H}_{85}\text{N}_{11}\text{O}_{14}\text{S}_2$  635.7854; found : 635.8154.

**Synthesis of BG-Cy3-Cy5.** To a solution of compound BG-Cy5 **5** (0.5 mg, 0.39  $\mu\text{mol}$ ,) in dry DMF (0.5 mL) were added Cy3-NHS ester (0.4 mg, 0.55  $\mu\text{mol}$ ) and  $\text{Et}_3\text{N}$  (1  $\mu\text{L}$ ) and the mixture was stirred overnight at room temperature. The product was purified by HPLC. Yield: 0.4 mg (54%) (determined by extinction coefficient of Cy5,  $\epsilon_{647} = 250,000 \text{ M}^{-1} \text{ cm}^{-1}$  in pH 7.4 buffer). MALDI (TOF):  $[\text{M}]^+$  calc for  $\text{C}_{93}\text{H}_{121}\text{N}_{13}\text{O}_{21}\text{S}_4$  1883.77; found 1883.79.

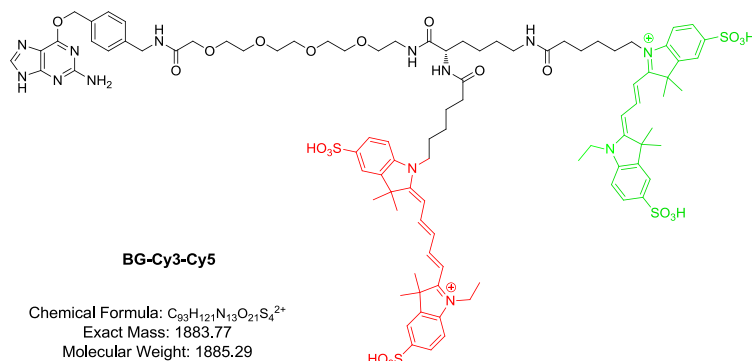


**Figure S2. Structure of BG-Cy3-Cy5.**

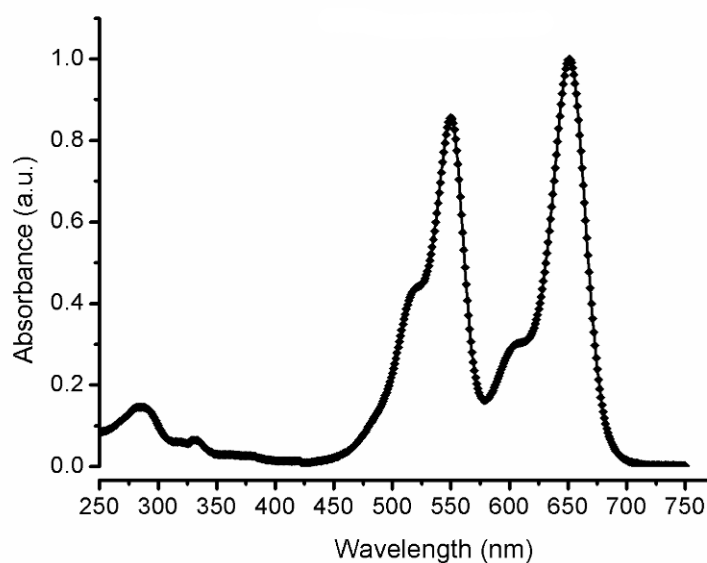


**Figure S3. Absorption spectrum of BG-Cy3-Cy5 (in HEPES, pH 7.4).**

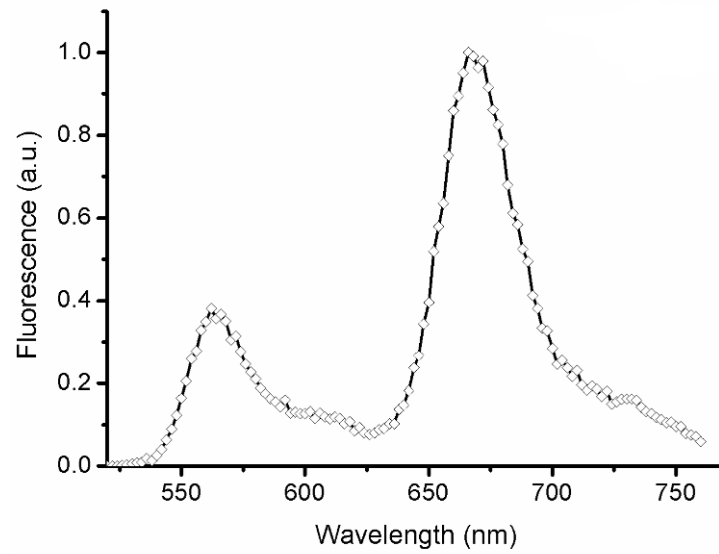


**Figure S4. Fluorescence emission spectrum of BG-Cy3-Cy5 (Ex. 500 nm) –(in HEPES, pH 7.4).**

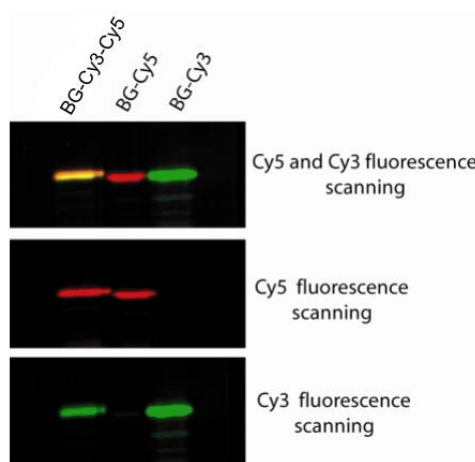


**Figure S5. Analysis of SNAP-tag reaction with BG-Cy3-Cy5 substrate by SDS-PAGE and fluorescence gel scanning. SNAP-GST (1  $\mu$ M) was incubated with 0.5  $\mu$ M of substrate for 2 h at room temperature in HEPES buffer (pH 7.4). SNAP-tag labeled with BG-Cy3 or BG-Cy5 were used as controls.**

## 2. Sample preparation for microscopy

**Cell fixation and staining.** 24 h after transfection, U2OS cells were rapidly extracted with 0.2% NP-40 in BRB80 (80 mM K-PIPES, pH 6.8, 1 mM MgCl<sub>2</sub>; 1 mM EGTA) pre-warmed to 37°C for 30 s,<sup>[3]</sup> followed by fixation with -20°C methanol containing 5 mM EGTA for 10 min.<sup>[4]</sup> Afterwards, cells were quickly washed 2-3 times with washing buffer (BRB80 or PBS (*Lonza*) supplemented with 1 mM EGTA and 1 mM MgCl<sub>2</sub>) and left overnight at 4°C in washing buffer containing 1% BSA.

For STORM experiments, SNAP-tagged<sup>[5]</sup> β-tubulin was labeled with 0.3 μM BG-Cy3-Cy5 in PBS containing 1% BSA for 1h at room temperature. The nuclei were stained by adding Hoechst 33342 stain to the same solution at 1 μg/ml concentration. The excess of dyes was removed by washing 3 times with washing buffer containing 0.05 % TX-100 reduced (*Sigma-Aldrich*) and leaving the samples overnight in the buffer at 4°C. A thin glass coverslip with cells was placed on a second glass slide with a drop of imaging buffer (50 HEPES pH 7.4, 50 mM NaCl or BRB80, 0.5 mg/ml glucose oxidase, 40 μg/ml catalase, 10% (w/v) glucose and 1% (v/v) β-mercaptoethanol) and sealed with nail polish just before STORM measurements.

**α-Tubulin immunostaining.** Immunostaining with mouse anti-α-tubulin was performed to confirm correct localization of SNAP-tagged β-tubulin. The primary mouse anti-α-tubulin antibody (DM1A, *Sigma-Aldrich*, 1:200 dilution in PBS with 1% BSA) was added to the samples and incubated overnight at 4°C. The samples were washed 3 times using washing buffer. After this, the secondary goat anti-mouse antibody labeled with Alexa488 (*Invitrogen*, 1:1000 dilution in PBS with 1% BSA) was added and incubated 1h at room temperature. Coverslips with cells were washed 3 times with washing buffer, placed on the glass slide with a drop of mounting medium (4% n-propyl-gallate, 90% glycerol in PBS) and sealed with nail polish before imaging.

**Plasmid.** Plasmid was a kind gift from Sun Luo (New England Biolabs). Human β-tubulin is cloned to the N-terminus of SNAP in pSEMS1-SNAP26m via ClaI and EcoRI sites.

### Abbreviations:

NP-40 is a commercially available detergent currently being replaced by Igepal CA-630 (*Sigma-Aldrich*)

BRB80 - "Brinkley Reassembly Buffer" or "Reassembly Buffer". Its composition is 80 mM K-PIPES, pH 6.8, 1 mM MgCl<sub>2</sub>; 1 mM EGTA

EGTA: ethyleneglycol tetraacetic acid

BSA: bovine serum albumin

PBS: phosphate buffer saline

HEPES: (4-(2-hydroxyethyl)-1-piperazineethanesulfonic acid )

K-PIPES: Piperazine-1,4-bis(2-ethanesulfonic acid) potassium salt

### 3. Image acquisition and processing

**Data acquisition.** The labeled samples were imaged using a custom designed inverted total internal reflection (TIRF) microscope in epi-illumination. The two laser excitation sources are a red HeNe laser (633 nm, 2.5mW) for imaging and a green Argon laser (514 nm, attenuated to 200  $\mu$ W) for activating the photoswitchable tags (Figure S6 and S7). The illumination area (beam waist) was approximately  $700 \mu\text{m}^2$ . For the STORM image reconstruction, 5000 images were acquired at a 20 Hz frame rate. A sample movie showing an extract of the image acquisition can be downloaded from the publisher's website.

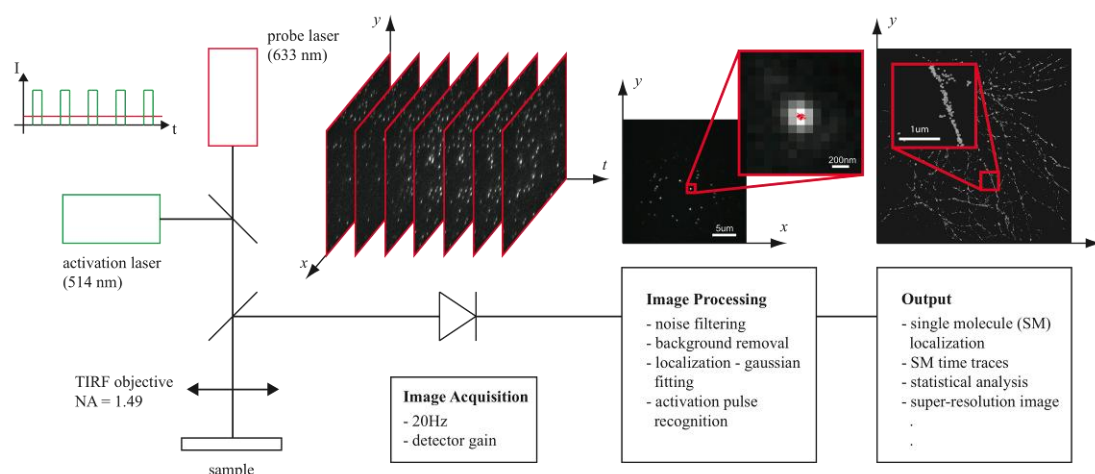


**Figure S6. Scheme of the setup, imaging and processing.**

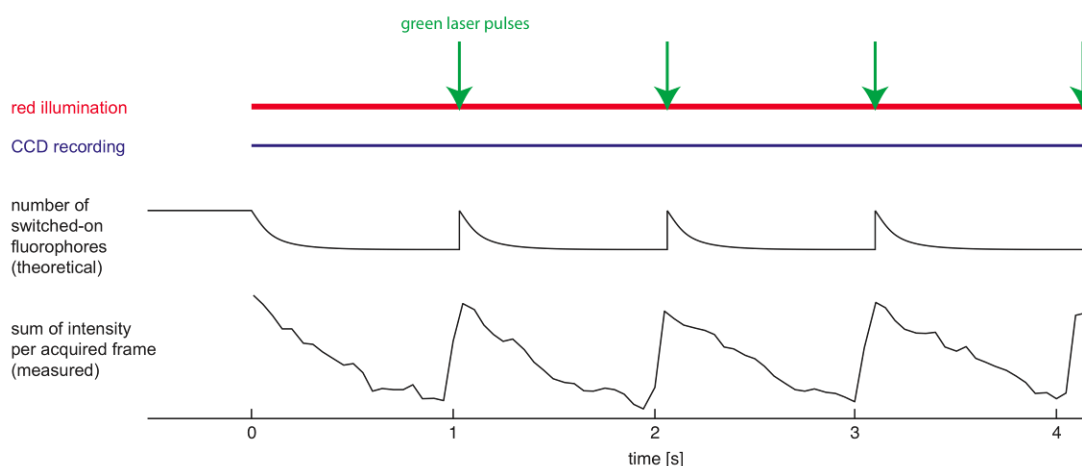


**Figure S7. Scheme of laser activation, signal recording and single fluorescence events.**

**Data analysis / software.** The image processing executed frame by frame is driven by a dedicated Matlab platform. The first step involves selecting and isolating spatially resolvable labeled molecules with sufficient intensity. To this end we apply a Laplacian of Gaussian filter ( $\sigma = 2.1$  pixel) in order to enhance the SNR of these single emission patterns and to suppress noise. In the following step, image segmentation with an adaptable threshold is

performed. Only segments with a size between 5 and 10 pixels are taken into account. The centre of gravity of the corresponding pixel values in the original image yields a first estimation of the fluorophore position. For the super-resolved images presented in this work, an improved accuracy is achieved by a Gaussian fit to the observed diffraction patterns. Outliers with a Gaussian amplitude smaller than 100 or higher than 1000, or a waist larger than 0.5  $\mu\text{m}$ , are rejected. The super-resolution image has a pixel matrix 10 times finer than the original acquired image. The pixel values correspond to the number of localized fluorophores within the enhanced pixel space.

**Sample drift correction.** During the whole image acquisition a small, but not negligible sample drift was observed. The blue line in Figure S8 shows the trace of an isolated molecule that was in a bright state during almost the whole sequence. This trace suggests a nearly linear sample drift throughout the acquisition. Therefore, the sample drift is corrected by shifting all localizations linearly as a function of time, this strongly improves the resulting super-resolution image. The required correction shift is estimated by relating the super-resolution image of the first 500 frames to the super-resolution image generated from the last 500 frames (red line in Figure S8).

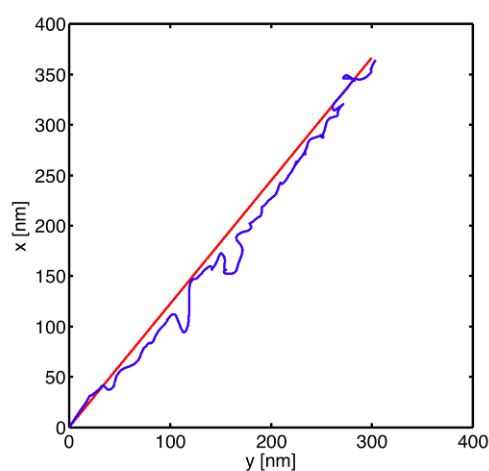


**Figure S8. Sample drift correction.** The blue line visualizes the sample drift based on tracking a single molecule. The red line represents the applied linear drift correction computed by means of a correlation between the super-resolution images based on the first 500 and the one of the last 500 frames.

**Image representation.** As shown in Figure S10, the wide field image, i.e. the corresponding pixel intensity  $I_{\text{wf}}$  is computed as

$$I_{\text{wf}} = \frac{1}{N} \sum_{n=1}^N \frac{I_n}{\max(I_n)}$$

where  $I_n$  is the n-th image frame of the STORM acquisition sequence and  $N$  the total number of frames. The displayed intensity  $I_{\text{disp}}$  of the super-resolution images corresponds to

$$I_{\text{disp}} = \ln(L_{\text{disp}} + p),$$

where  $L_{\text{disp}}$  are the number of localizations per refined pixel and  $p = 1$  an offset. The refined pixel size corresponds to 10 nm according to the expected localization accuracy.

**Resolution and expected localization accuracy.** The localization accuracy is measured by tracking an isolated single emitter that was in a bright state during almost the whole image acquisition. After linear drift correction, the standard deviation of the localizations is  $\sigma = 11.3\text{nm}$ . An estimation considering the different noise sources can also be computed by the following expression:<sup>[6]</sup>

$$\sigma^2 = \langle(\Delta x)^2\rangle = \frac{s^2 + a^2/12}{N} + \frac{8\pi s^4 b^2}{a^2 N^2}$$

where  $b = 25$  represents the standard deviation of the background measured in an empty area with no emitters and  $a = 100$  nm is the effective pixel size taking into account the magnification of the microscope.  $N = 2\pi A (s/a)^2 / c$  is the number of collected photons per molecule and is computed according to the peak values in Figure S9 with  $c = 5$  a pixel - photon count conversion factor,  $s = 120$  nm the waist and  $A = 250$  the amplitude of the Gaussian in the localization algorithm. We find  $\sigma = 9.9$  nm, which underestimates the measured uncertainty as expected by R. E. Thompson.<sup>[6]</sup> In addition, this is also due to the not fully compensated drift in the measured standard deviation.

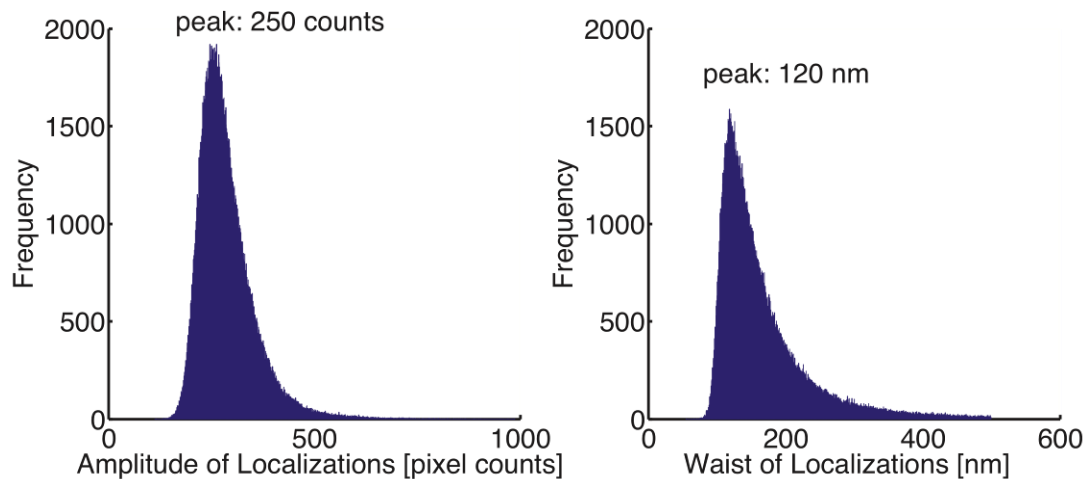


**Figure S9. Distribution of amplitude and waist of the Gaussian fit.** Most of the localizations have a Gaussian amplitude of about  $A = 250$  pixel counts and a waist of about  $s = 120\text{nm}$ .

The full width half maximum (FWHM) of the localization distribution can be interpreted as the achieved resolution. We find

$$\text{FWHM} = 2\sqrt{2\ln(2)} \sigma \approx 25 \text{ nm}$$

**Noise suppression.** Single emitter localizations not connected to others have been removed with the function “remove outliers” of radius 0 and threshold 1 using the freeware “*ImageJ*”.

**Bleaching.** In order to avoid bleaching of the sample, the sample was observed in a sealed chamber and an oxygen scavenging system was added to the imaging buffer. The ensemble intensity of the sample lowers only to 97% over 60 reactivation cycles.

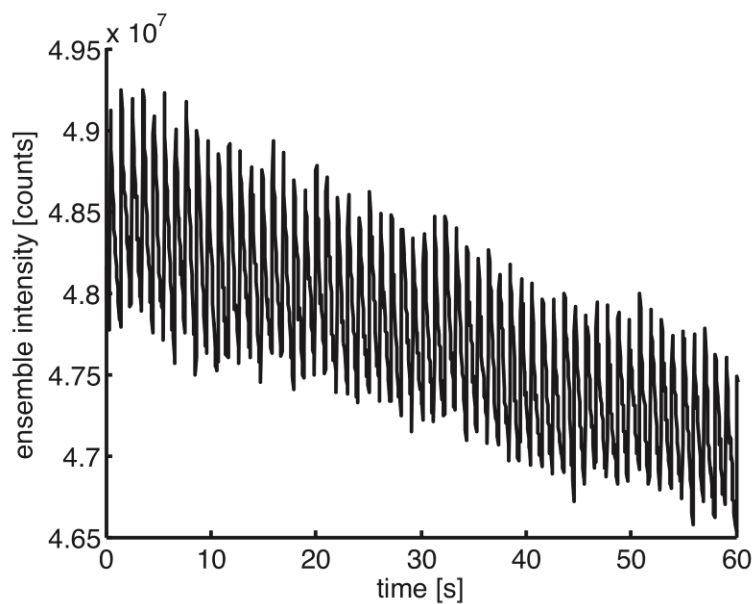


**Figure S10. Decreasing ensemble intensity of the sample due to bleaching.** The oscillations are due to the reactivation molecules.

**Kinetic trace of a single molecule.**

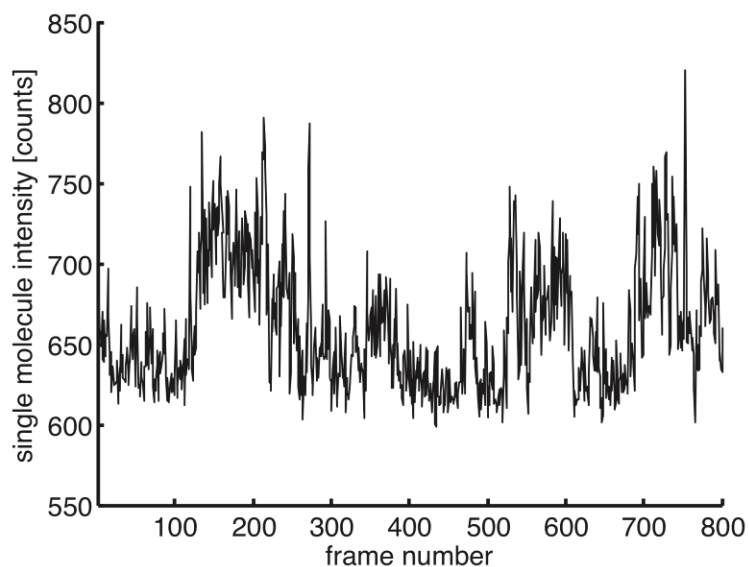


**Figure S11. Kinetic trace of a BG-Cy3-Cy5.**

#### 4. Comparison of resolution between confocal and STORM images

The imaging improvement due to STORM imaging becomes apparent by comparing microtubule structures imaged with a state of the art confocal microscope and the calculated STORM image. The width of the Gaussian fit to each of the cross sections in Figure S12 e) and f) demonstrates directly the improvement by almost an order of magnitude.

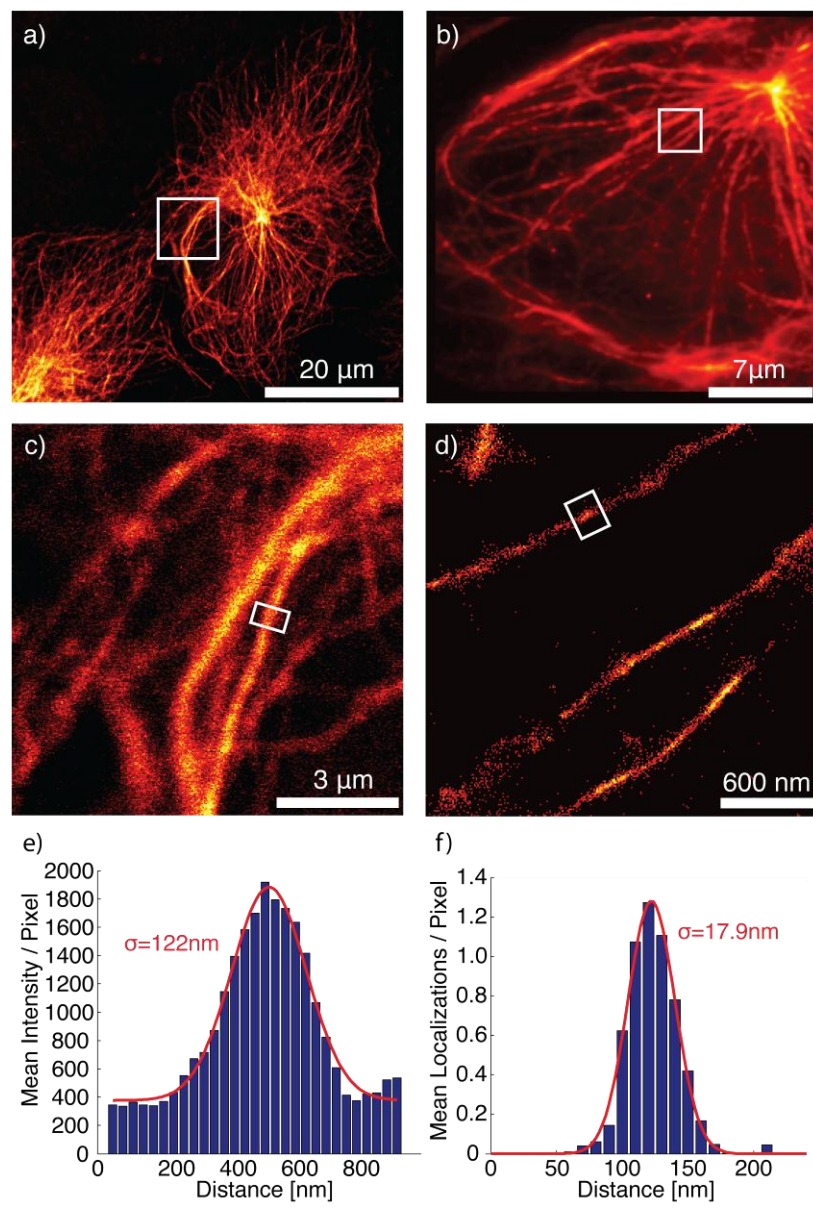


**Figure S12. Confocal images (left side) and STORM images (right side).** a) confocal image of two U2OS cells (marker BG-Cy3-Cy5). b) wide field image of a U2OS cell given by the sum of all frames of the STORM acquisition. c) zoom-in to the white square in a). d) STORM image of the white square in b). e) transversal cross section of the tubuline structure in the white rectangle in c) along with a Gaussian fit. The cross section is averaged over a 660nm large region along the structure. f) transversal cross section of the tubuline structure in the white rectangle in d) along with a Gaussian fit. The cross section is averaged over a 200nm large region along the structure.

## 5. Supporting references

- [1] S. Banala, A. Arnold, K. Johnsson, *ChemBioChem* **2008**, *9*, 38.
- [2] J. T. Lundquist, J. C. Pelletier, *Org. Lett.* **2002**, *4*, 3219.
- [3] M. Piel, P. Meyer, A. Khodjakov, C. L. Rieder, M. Bornens, *J Cell Biol* **2000**, 317.
- [4] M. Osborn, K. Weber, *Methods Cell Biol* **1982**, *24*, 97.
- [5] a) A. Keppler, S. Gendreizig, T. Gronemeyer, H. Pick, H. Vogel, K. Johnsson, *Nat Biotechnol* **2003**, *21*, 86; b) A. Keppler, M. Kindermann, S. Gendreizig, H. Pick, H. Vogel, K. Johnsson, *Methods* **2004**, *32*, 437; c) A. Keppler, H. Pick, C. Arrivoli, H. Vogel, K. Johnsson, *Proc Natl Acad Sci U S A* **2004**, *101*, 9955.
- [6] R. E. Thompson, D. R. Larson, W. W. Webb, *Biophysical Journal* **2002**, *82*, 2775.